The Canadian Mineralogist
Vol. 40, pp. 509-517 (2002)

THE SYSTEM Fe–Pt–S AT 1100°C

JURAJ MAJZLAN

Department of Geology, University of California at Davis, Davis, California 95616, U.S.A.

MILOTA MAKOVICKY, EMIL MAKOVICKY[§] AND JOHN ROSE-HANSEN

Geological Institute, University of Copenhagen, Øster Voldgade 10, DK–1350 Copenhagen K, Denmark

ABSTRACT

The system Fe–Pt–S at 1100°C contains four alloys, γ(Fe,Pt), PtFe, Pt_3Fe and γ(Pt, Fe), with respective miscibility-gaps at 43.5–45.5 at.% Pt, 57.7–60.4 at.% Pt and 77–80 at.% Pt, two sulfide phases, $Fe_{1-x}S$ (maximum Pt solubility 1.1 at.% at 54.3 at.% S) and PtS (0.5–0.8 at.% Fe maximum), a Fe-rich sulfide melt (Pt solubility below microprobe limits) and a S-rich sulfide melt (Pt solubility 7.5 at.% for solidified melts with ~54.5 at.% S). Of the five two-phase and five three-phase associations, the most important are PtFe – Pt_3Fe – $Fe_{1-x}S$ (Pt below detection), Pt_3Fe – $Fe_{1-x}S$ (0.4 at.% Pt) – PtS, Pt_3Fe – γ(Pt,Fe) – PtS and $Fe_{1-x}S$ (0.9 at.% Pt) – melt (~8.5 at.% Pt) – PtS. Comparisons of experimental data with natural associations enable us to suggest several genetic and geothermometric implications.

Keywords: system Fe–Pt–S, iron–platinum alloys, isoferroplatinum, monosulfide solid-solution, cooperite.

SOMMAIRE

Le système Fe–Pt–S à 1100°C contient quatre alliages, γ(Fe,Pt), PtFe, Pt_3Fe et γ(Pt, Fe), ayant des lacunes de miscibilité à 43.5–45.5% Pt, 57.7–60.4% Pt et 77–80% Pt (proportions atomiques), deux sulfures, $Fe_{1-x}S$ (solubilité maximale de Pt 1.1% à 54.3% de S) et PtS (teneur maximale en fer 0.5–0.8%), un bain fondu sulfuré enrichi en Fe (la solubilité du Pt y est inférieure au seuil de détection) et un bain fondu riche en S (la solubilité maximale du Pt y est de 7.5% pour les liquides solidifiés contenant ~54.5% S). Des cinq associations à deux phases et cinq associations à trois phases, les plus importantes seraient PtFe – Pt_3Fe – $Fe_{1-x}S$ (teneur en Pt inférieure au seuil de détection), Pt_3Fe – $Fe_{1-x}S$ (0.4% Pt) – PtS, Pt_3Fe – γ(Pt,Fe) – PtS et $Fe_{1-x}S$ (0.9% Pt) – melt (~ 8.5% Pt) – PtS. En comparant les données expérimentales avec les associations naturelles, nous sommes en mesure d'évaluer plusieurs implications génétiques et géothermométriques.

(Traduit par la Rédaction)

Mots-clés: système Fe–Pt–S, alliages fer–platine, isoferroplatine, solution solide monosulfurée, cooperite.

INTRODUCTION

The system Fe–Pt–S is one of the most important ones with respect to the genesis of platinum-group-element (PGE) ore deposits. The 500° and 900°C isothermal sections were studied by Makovicky *et al.* (1988), and the 1000°C section by Skinner *et al.* (1976). Additional data can be extracted from the study of the system Pt–Fe–As–S at 470° and 850°C by Makovicky *et al.* (1992).

Bryukvin *et al.* (1985) documented the eutectic in the system Pt–PtS, and Bryukvin *et al.* (1987) described the melting relations in the system Fe–$FeS_{1.09}$–Pt–PtS. The mineralogy of Pt–Fe alloys was worked out by Cabri & Feather (1975). The most recent substantial contributions to their mineralogy were made by Bowles (1990) and Cabri *et al.* (1996). The present contribution completes this information by describing the phase relationships in the system Fe–Pt–S just below the eutectic temperature, at 1100°C. The data have implications for the genesis of PGE deposits.

EXPERIMENTAL

Thirty-six 150 mg charges were weighted out from pure elements. They were sealed in evacuated silica glass tubes, preheated at 300°C and annealed for a week at 1100°C. Those charges that were melt-free were

§ *E-mail address*: emilm@geo.geol.ku.dk

reground and homogenized, and they were then resealed and re-annealed. The polished samples were investigated in reflected polarized light and characterized by electron-microprobe analysis. A JEOL Superprobe 733 was used in wavelength-dispersion mode, with an on-line correction program supplied by JEOL. Wavelengths employed were Fe$K\alpha$, S$K\alpha$ and Pt$L\alpha$. Natural chalcopyrite and Pt metal served as the microprobe standards. Frequently repeated measurements of the standards enabled normalization of the microprobe results. The excitation voltage was 20 kV, beam current 30 nA, beam diameter 1–2 μm and the counting time up to 20 s. Homogeneous solid phases were analyzed by means of point analyses; solidified melts and finely exsolved solid-solutions were characterized by means of a sweeping electron beam at 10000× magnification, and the results from a number of randomly selected areas were averaged. The detection limit of the microprobe technique is 0.05 wt.% Fe, 0.17% S and 0.08% Pt.

The sulfur-rich melts solidified while boiling off sulfur in excess of mineral compositions of the resulting sulfide mixture (primarily $Fe_{1-x}S$), and thus yielded S contents lower than the original bulk composition, and occasionally also a vesicular texture. The original compositions of the melt phase were obtained from intersections of the line (Pt,Fe)S – bulk-charge composition with the Fe/Pt line relevant to the solidified melt. Of course, this method cannot delineate the S-rich boundary of the field of melt; this boundary remains conjectural because it is not possible to discern unambiguously the primary and secondary free sulfur in the charge.

Phase relations

At 1100°C, the system Fe–Pt–S contains two sulfide phases, two melts and four alloys (Fig. 1). Electron-microprobe results used are listed in Table 1. The S-poor portion of the system is occupied by five two-phase and five three-phase associations (empirical microprobe-derived compositions, all data in at.%):

1) γ(Fe,Pt) – (Fe,S) melt, typified by the join ($Fe_{81.2}Pt_{18.8}$) – ($Fe_{53.3}Pt_{0.0}S_{46.7}$),

2) γ(Fe,Pt) ($Fe_{68.8}Pt_{31.2}$) – (Fe,S) melt ($Fe_{51.8}Pt_{0.0}S_{48.2}$) – $Fe_{1-x}S$ ($Fe_{49.5}Pt_{0.0}S_{50.5}$),

3) γ(Fe,Pt) – $Fe_{1-x}S$, *e.g.*, ($Fe_{63.2}Pt_{36.8}$) – ($Fe_{49.3}Pt_{0.0}S_{50.7}$),

4) γ(Fe,Pt) ($Fe_{56.5}Pt_{43.5}$) – PtFe ($Fe_{54.5}Pt_{45.5}$) – $Fe_{1-x}S$ ($Fe_{49.4}Pt_{0.0}S_{50.6}$),

5) PtFe ($Fe_{42.3}Pt_{57.7}$) – Pt_3Fe ($Fe_{39.6}Pt_{60.4}$) – $Fe_{1-x}S$ ($Fe_{48.2}Pt_{0.0}S_{51.8}$),

6) Pt_3Fe – $Fe_{1-x}S$, typified by ($Fe_{35.9}Pt_{64.1}$) – ($Fe_{48.4}S_{51.6}$),

7) Pt_3Fe ($Fe_{26.1}Pt_{73.9}$) – $Fe_{1-x}S$ ($Fe_{46.7}Pt_{0.4}S_{52.9}$) – PtS (0.54 Fe), flanked by the binary Pt_3Fe – $Fe_{1-x}S$ and Pt_3Fe – PtS associations,

8) Pt_3Fe ($Fe_{23}Pt_{77}$) – γ(Pt,Fe) ($Fe_{20}Pt_{80}$) – PtS (0.1–0.2 Fe) (Makovicky & Karup-Møller 2000)

9) γ(Pt,Fe) – PtS, typified by ($Fe_{12.2}Pt_{87.8}$) – PtS (0.08 Fe).

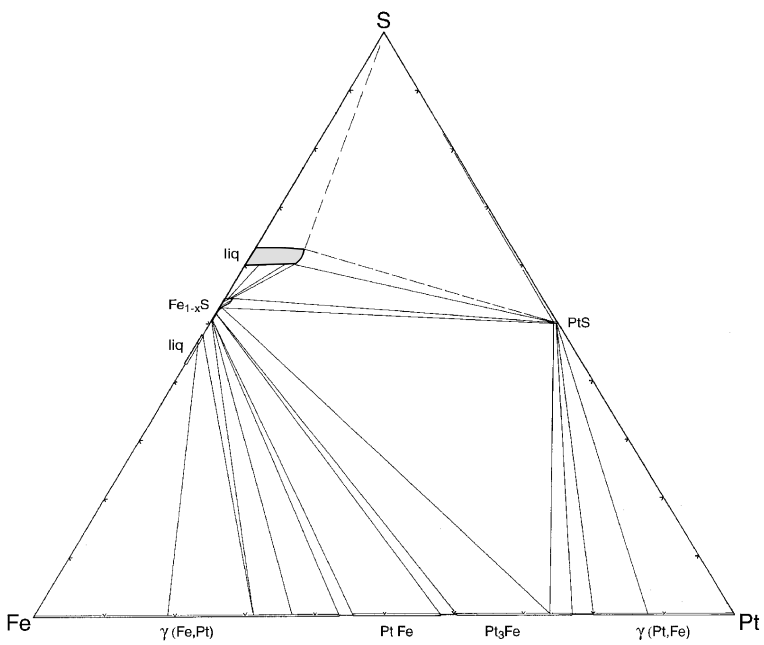

FIG. 1. Phase diagram for the system Fe–Pt–S at 1100°C.

TABLE 1. SELECTED RUNS IN THE SYSTEM Fe–Pt–S AT 1100°C

Run no.	Phase	S	Fe	Pt	Total	No. meas.	Fe	S	Pt
		wt.%					at.%		
1	alloy	0.09	60.26	39.74	100.11	15	83.94	0.22	15.85
		0.06	3.38	3.49			4.71	0.15	1.39
	liq	34.17	65.62	0.04	99.85	15	52.43	47.56	0.01
		2.93	3.39	0.05			2.71	4.08	0.01
3	alloy	0.08	38.68	61.17	99.93	6	68.67	0.25	31.09
		0.07	1.10	0.99			1.95	0.22	0.50
	liq	34.61	64.83	0.03	99.50	11	51.81	48.18	0.01
		2.75	2.92	0.02			2.33	3.83	0.01
	po	36.97	63.11	0.08	100.18	8	49.49	50.49	0.02
		0.30	0.42	0.10			0.33	0.41	0.03
4	alloy	0.12	32.88	66.99	100.01	11	62.91	0.40	36.69
		0.06	0.28	0.31			0.54	0.20	0.17
	po	36.95	62.52	0.05	99.54	14	49.27	50.72	0.01
		0.28	0.47	0.07			0.37	0.38	0.01
6	alloy	0.16	13.70	85.64	99.52	14	35.59	0.72	63.69
		0.10	0.22	0.70			0.57	0.45	0.52
	po	37.76	61.79	0.06	99.63	6	48.43	51.55	0.01
		0.30	0.47	0.06			0.37	0.41	0.01
7	PtS	14.50	0.30	84.79	99.60	7	0.60	50.69	48.71
		0.25	0.03	0.47			0.06	0.87	0.27
	po	38.90	59.36	1.57	99.86	6	46.53	53.11	0.35
		0.29	0.26	0.32			0.20	0.40	0.07
	alloy	0.12	9.47	91.08	100.68	6	26.49	0.58	72.93
		0.06	0.24	0.33			0.67	0.29	0.26
8	alloy	0.10	8.97	90.83	99.92	8	25.52	0.50	73.98
		0.07	0.13	0.46			0.37	0.35	0.37
	PtS	14.63	0.25	85.68	100.58	7	0.50	50.70	48.80
		0.35	0.04	0.23			0.08	1.21	0.13
	po	38.81	59.25	1.54	99.61	6	46.55	53.11	0.35
		0.29	0.23	0.10			0.18	0.40	0.02
9	alloy	0.10	24.98	72.89	97.96	2	54.28	0.38	45.34
		0.12	0.01	0.49			0.02	0.46	0.30
	po	36.79	62.47	0.15	99.43	6	49.35	50.62	0.03
		0.18	0.21	0.10			0.17	0.25	0.02
	alloy	0.10	27.00	72.63	99.74	6	56.29	0.36	43.35
		0.08	0.30	0.35			0.63	0.29	0.21
10	po	37.91	61.35	0.12	99.40	6	48.15	51.82	0.03
		0.38	0.32	0.10			0.25	0.52	0.03
	alloy	0.20	17.02	81.20	98.43	4	41.91	0.86	57.23
		0.13	0.26	0.26			0.64	0.56	0.18
	alloy	0.19	15.57	83.00	98.77	7	39.26	0.83	59.91
		0.10	0.10	0.47			0.25	0.44	0.34
11	po	38.86	59.46	1.52	99.88	8	46.61	53.05	0.34
		0.41	0.37	0.36			0.29	0.56	0.08
	alloy	0.16	9.19	91.08	100.44	9	25.84	0.79	73.36
		0.10	0.69	0.55			1.94	0.49	0.44
	PtS	14.38	0.25	85.06	99.70	1	0.50	50.45	49.05
12	po	38.68	59.08	1.37	99.18	9	46.58	53.11	0.31
		0.21	0.44	0.32			0.35	0.29	0.07
	alloy	0.14	9.06	90.69	99.90	7	25.69	0.69	73.62
		0.07	0.18	0.40			0.51	0.34	0.32
	PtS	14.38	0.24	85.19	99.82	8	0.48	50.42	49.09
		0.15	0.03	0.21			0.06	0.53	0.12
13	po	38.40	59.67	1.47	99.58	12	46.99	52.67	0.33
		0.27	1.13	0.13			0.89	0.37	0.03
	PtS	14.58	0.24	86.18	101.02	8	0.48	50.48	49.04
		0.15	0.03	0.66			0.06	0.52	0.38
	alloy	0.16	9.30	90.98	100.46	8	26.11	0.78	73.11
		0.05	0.20	06.9			0.56	0.24	0.55
15	PtS	14.53	0.04	85.26	99.85	8	0.08	50.86	49.05
		0.25	0.02	0.90			0.04	0.88	0.52
	alloy	0.15	3.81	95.76	99.74	17	12.10	0.83	87.07
		0.07	0.85	1.26			2.70	0.39	1.15
16	po	38.87	60.40	1.63	100.93	7	46.98	52.66	0.36
		0.45	0.45	0.26			0.35	0.61	0.06
	PtS	14.49	0.25	85.69	100.44	7	0.50	50.46	49.04
		0.26	0.02	0.34			0.04	0.91	0.19
	alloy	0.16	9.29	90.94	100.41	8	26.09	0.78	73.12
		0.06	0.12	0.75			0.34	0.29	0.60
17	liq	33.12	69.39	0.14	102.69	8	54.59	45.38	0.03
		1.16	1.34	0.08			1.05	1.59	0.02
	alloy	0.10	48.72	50.67	99.50	5	76.85	0.27	22.88
		0.08	0.46	0.42			0.73	0.22	0.19
18	alloy	0.10	49.26	50.64	100.01	7	77.05	0.27	22.68
		0.07	0.42	0.76			0.66	0.19	0.34
	liq	34.10	68.21	0.03	102.37	8	53.45	46.54	0.01
		2.38	2.26	0.02			1.77	3.25	0.01
19	po	39.72	57.68	3.91	101.34	9	45.07	54.06	0.87
		0.25	0.44	0.32			0.34	0.34	0.07
	PtS	14.53	0.23	85.89	100.67	8	0.46	50.49	49.05
		0.32	0.05	0.98			0.10	1.11	0.56
20	po	39.65	57.96	4.10	101.75	8	45.21	53.87	0.92
		0.25	0.25	0.13			0.20	0.34	0.03
	PtS	14.66	0.23	85.85	100.76	8	0.46	50.72	48.82
		0.32	0.07	0.25			0.14	1.11	0.14
21	PtS	14.67	0.36	85.83	100.89	8	71	50.62	48.67
		0.21	0.06	0.58			0.12	0.72	0.33
	po	39.00	59.59	1.69	100.30	12	46.55	53.07	0.38
		0.37	0.70	0.16			0.55	0.50	0.04
	alloy	0.11	8.75	90.98	99.85	3	25.02	0.53	74.45
		0.09	0.73	0.69			2.09	0.43	0.56
21x	po	39.83	57.50	4.50	101.85	10	44.87	54.13	1.01
		0.40	0.28	0.23			0.22	0.54	0.05
	PtS	14.60	0.25	85.10	99.96	8	0.50	50.82	48.68
		0.26	0.09	0.44			0.18	0.91	0.25
22	po	39.63	57.80	4.99	102.45	8	45.07	53.82	1.11
		0.24	0.65	0.34			0.51	0.33	0.08
	PtS	14.48	0.24	85.36	100.11	5	0.48	50.55	48.97
		0.34	0.09	0.73			0.18	1.19	0.42
PTN-1	PtS	14.26	0.20	85.77	100.22	7	0.41	50.09	49.50
		0.19	0.05	0.62			0.10	0.67	0.36
	liq	33.65	40.77	26.21	100.63	36	38.14	54.84	7.02
		0.99	1.88	2.54			1.76	1.61	0.68
PTN-2	PtS	14.43	0.21	85.20	99.83	8	0.42	50.53	49.05
		0.14	0.05	0.43			0.10	0.49	0.25
	liq	33.98	39.93	26.24	100.15	34	37.45	55.51	7.04
		1.27	2.32	3.56			2.18	2.07	0.96
PTN-3	PtS	14.42	0.25	85.82	100.49	10	0.50	50.30	49.19
		0.35	0.04	0.25			0.08	1.22	0.14
	liq	34.59	41.62	24.60	100.81	37	38.22	55.32	6.47
		1.86	3.18	4.61			2.92	2.97	1.21
PTN-4	PtS	14.31	0.26	85.25	99.81	9	0.52	50.27	49.21
		0.16	0.04	0.42			0.08	0.56	0.24
	liq	33.56	41.01	26.46	101.03	41	38.31	54.61	7.08
		1.27	2.05	2.76			1.92	2.07	0.74
PTN-5	PtS	14.63	0.28	85.75	100.65	10	0.55	50.64	48.81
		0.13	0.04	0.30			0.08	0.45	0.17
	liq	34.31	40.90	25.91	101.12	41	37.84	55.29	6.86
		1.44	2.47	3.81			2.29	2.32	1.01
PTN-6	PtS	14.21	0.24	85.57	100.02	15	0.49	50.02	49.49
		0.20	0.05	0.36			0.10	0.70	0.21
	liq	34.88	40.04	25.86	100.78	32	37.01	56.15	6.84
		0.75	1.23	1.50			1.14	1.21	0.40
PTN-7	PtS	14.13	0.25	85.43	99.81	9	0.51	49.91	49.59
		0.33	0.05	0.76			0.10	1.17	0.44
	liq	33.77	40.21	26.18	100.17	34	37.75	55.22	7.04
		1.18	2.11	3.22			1.98	1.93	0.87
PTN-8	PtS	13.97	0.26	85.55	99.77	13	0.53	49.58	49.89
		0.32	0.06	0.41			0.12	1.14	0.24
	liq	33.73	41.62	24.94	100.29	35	38.71	54.65	6.64
		0.79	1.77	2.26			1.65	1.28	0.60
PTN-9	PtS	14.26	0.23	85.52	99.99	10	0.46	50.12	49.41
		0.17	0.05	0.38			0.10	0.60	0.22
	liq	34.00	40.06	26.24	100.30	34	37.51	55.45	7.03
		1.51	2.72	4.31			2.55	2.46	1.15
PTN-10	PtS	14.14	0.26	85.29	99.68	14	0.52	49.95	49.53
		0.28	0.04	0.62			0.08	0.99	0.36
	liq	33.80	41.03	24.81	99.65	28	38.34	55.02	6.64
		1.08	1.66	2.43			1.55	1.76	0.65
11-A	po	39.88	57.61	3.06	100.59	17	45.02	54.27	0.69
		0.37	0.47	0.48	0.60		0.37	0.50	0.11
	liq	39.61	53.64	7.76	101.03	10	42.96	55.25	1.78
		0.56	1.72	2.41	0.51		1.38	0.78	0.55
	po	39.73	56.94	4.01	100.71	13	44.72	54.35	0.90
		0.66	1.07	1.45	1.08		0.84	0.90	0.33
	liq	39.20	53.95	9.63	102.82	20	43.15	54.62	2.21
		1.20	3.34	4.98	1.16		2.67	1.67	1.14

TABLE 1. SELECTED RUNS IN THE SYSTEM Fe–Pt–S AT 1100°C

Run no.	Phase	S	Fe	Pt	Total	No. meas.	Fe	S	Pt
		wt.%					at.%		
11-B	PtS	14.73	0.42	85.40	100.57	11	0.83	50.75	48.37
		0.24	0.23	0.37	0.40		0.45	0.83	0.21
	po	39.49	56.57	4.49	100.59	10	44.65	54.29	1.01
		0.37	0.28	0.41	0.59		0.22	0.51	0.09
	liq	34.19	41.61	26.52	102.36	14	38.25	54.73	6.98
		0.76	1.14	1.49	0.67		1.05	1.22	0.39
11-C	PtS	14.75	0.31	85.30	100.38	12	0.61	50.95	48.41
		0.27	0.09	0.40	0.54		0.18	0.93	0.23
	po	39.48	57.83	3.84	101.19	2	45.28	53.84	0.86
		0.23	0.29	0.13	0.11		0.23	0.31	0.03
	po	39.86	57.25	3.88	101.04	15	44.79	54.31	0.87
		0.24	0.80	1.11	0.73		0.63	0.33	0.25
11-D	PtS	14.58	1.15	84.74	100.47	4	2.25	49.97	47.75
	near po	0.15	0.40	0.84	0.79		0.78	0.51	0.47
	PtS	14.63	0.28	85.33	100.26	13	0.57	50.74	48.66
	crystals	0.13	0.11	0.32	0.24		0.22	0.45	0.18
	po	39.95	56.81	3.61	100.40	29	44.57	54.29	0.81
		0.42	0.76	0.87	0.97		0.60	0.57	0.20
11-E	PtS	14.70	0.29	85.39	100.40	15	0.59	50.84	48.55
		0.19	0.16	0.54	0.55		0.33	0.66	0.31
	PtS	14.58	0.88	85.19	100.68	2	1.73	50.11	48.11
	near liq	0.04	0.02	0.25	0.25		0.04	0.14	0.14
	liq	33.49	39.87	27.72	101.12	20	37.56	54.94	7.47
		1.49	1.95	3.17	1.31		1.84	2.44	0.85
	coarse	34.89	42.67	23.80	101.40	3	38.69	55.10	6.18
	liq	0.61	2.42	3.66	0.77		2.19	0.96	0.95
11-F	PtS	14.66	0.28	85.31	100.27	16	0.55	50.82	48.59
	near po	0.30	0.17	0.41	0.62		0.33	1.04	0.23
	liq	33.28	40.88	27.34	101.52	15	38.32	54.33	7.33
		0.73	1.02	1.56	0.71		0.96	1.19	0.42
11-G	po	39.59	57.92	2.78	100.32	14	45.35	54.00	0.62
		0.24	0.69	0.45	0.55		0.54	0.33	0.10
	po	39.28	58.07	3.07	100.46	9	45.58	53.71	0.69
		0.41	0.47	0.75	0.57		0.37	0.56	0.17
	liq	35.01	45.12	21.04	101.19	13	40.24	54.38	5.37
		2.08	3.95	5.51	1.35		3.52	3.23	1.41
11-H	liq	31.66	37.83	30.09	99.61	11	37.23	54.27	8.48
		2.08	3.57	3.94	2.73		3.51	3.57	1.11
	po	39.96	58.13	2.80	100.90	3	45.22	54.14	0.62
		0.65	0.27	0.14	0.47		0.21	0.88	0.03
	po	39.70	57.18	3.85	100.75	11	44.86	54.25	0.86
		0.33	0.68	0.43	0.52		0.53	0.45	0.10
eutectic liquid*		33.13	39.31	27.95	100.38	16	37.43	54.95	7.62
		0.66	0.99	1.17			0.94	1.09	0.32
po dendrites*		40.48	55.29	3.47	99.26	6	43.61	55.61	0.78
		0.27	0.47	0.63			0.37	0.37	0.14

* Quench products.

The phase Fe_3Pt, known from the system Pt–Fe, is not stable above ~850°C, where it disorders and transforms to γ(Fe,Pt) (Kubaschewski 1982).

The S-rich portion of the system is occupied by the following assemblages (liquid compositions were corrected for the loss of sulfur):

1) PtS (0.5–0.8 at.% Fe) – $Fe_{1-x}S$ ($Fe_{45.3}Pt_{0.9}S_{53.8}$ to $Fe_{44.7}Pt_{1.1}S_{54.3}$),

2) PtS – (S,Fe,Pt) melt $Fe_{32.4}Pt_{7.4}S_{60.2}$ – $Fe_{1-x}S$ ($Fe_{44.9}Pt_{0.9}S_{54.3}$) (charge A in Table 1),

3) PtS (0.6 Fe) – (S,Fe,Pt) melt; melt triangulated as $Fe_{32.2}Pt_{6.4}S_{61.4}$ (charge E in Table 1) and $Fe_{33.1}Pt_{6.3}S_{60.6}$ (F),

4) PtS (0.4 Fe) – (S,Fe,Pt) melt (triangulated as $Fe_{31.7}Pt_{5.8}S_{62.5}$) – S,

5) $Fe_{1-x}S$ – (S,Fe,Pt) melt; typified by the tie-lines $Fe_{44.7}Pt_{0.9}S_{54.4}$ – melt, the composition of which was recalculated as $Fe_{37.9}Pt_{1.9}S_{60.2}$, and $Fe_{45.6}Pt_{0.7}S_{53.7}$ – melt, with the composition recalculated as $Fe_{35.1}Pt_{4.7}S_{60.2}$,

6) (S,Fe,Pt) melt – S,

7) PtS – S.

PtS_2, still reported in the system Fe–Pt–S at 900°C (Makovicky *et al.* 1988), was not encountered in this study, nor was it found in the isothermal section of the system at 1000°C (Skinner *et al.* 1976). The upper stability limit of PtS_2 is unknown.

Phase composition

The Pt–Fe join of the system is characterized by a field of Pt–Fe alloys whose composition varies almost without interruptions over the entire range from Fe to Pt. Our data gave very good estimates for two out of the three narrow miscibility-gaps separating the four Pt–Fe alloys. The empirical sulfur content in these alloys is low (< 0.29 wt.%) and fully comparable to spurious sulfur values detected in the pure Pt standard. The third miscibility gap is taken from the study of the Fe–Pt–Ir–S system by Makovicky & Karup-Møller (2000). The sluggish rates of reaction prevented equilibration of the samples close to the Pt apex, even at this high temperature of annealing. In the samples positioned centrally in the system, two coexisting Pt–Fe alloys are readily observed in reflected polarized light because PtFe is weakly anisotropic, whereas all the other alloys are isotropic. Coexisting alloys form intimate intergrowths of lath-like grains, being in contact with each other and also with the surrounding $Fe_{1-x}S$. Compositions of the Pt–Fe alloy in the three-phase assemblage Pt_3Fe – PtS – $Fe_{1-x}S$ are tightly clustered around the empirical composition $Fe_{26.1(11)}Pt_{73.9(4)}$ (average of seven independent runs; numbers in brackets are standard deviations in terms of the last digit).

PtS dissolves minor amounts of Fe in all the phase assemblages. The electron-microprobe results do not

deviate significantly from the stoichiometric *Me*/S ratio. In a single two-phase assemblage PtS – γ(Pt,Fe) observed in our study, an average of 0.08 at.% Fe (*i.e.*, close to the detection limit) present in PtS is associated with alloy of a broad average composition $Fe_{12.2(27)}Pt_{87.8(16)}$. Makovicky & Karup-Møller (2000) reported 0.1–0.2 (exceptionally 0.5) at.% Fe (and <0.1–0.2 at.% Ir) in PtS in the ternary association of PtS with γ(Pt,Fe) and Pt_3Fe in the system Fe–Ir–Pt–S. In the present study, PtS coexisting with Pt_3Fe and pyrrhotite contains 0.5–0.7 at.% Fe.

The PtS crystals from the ternary association PtS – S-rich melt – S were not found to be chemically homogeneous. They show a thin Fe-rich rim (up to 1.96 at.% Fe) and a Fe-poor core (0.36 at.% Fe). The enrichment of Fe in the rim is attributed to crystallization of surface layers from the surrounding melt during quenching. These results are not included in the overall average. The Fe content in PtS exclusive of rims and innermost cores was found to vary between 0.41 and 0.55 at.% and is interpreted as the product of equilibrium crystallization at 1100°C.

The (Fe,S) melt (iron-rich sulfide melt) was analyzed by sweeping the electron beam over randomly selected areas. Its Pt concentration is below the detection limit of the electron microprobe. On quenching, it always yields dendrites of iron monosulfide and a eutectic mixture of γFe and near-stoichiometric FeS. Therefore, its composition must have been richer in S than the eutectic composition ($Fe_{55.4}S_{44.6}$) known in the Fe–S system (Kubaschewski 1982) in all runs shown in Table 1. Clusters of single analytical compositions start at the Fe-rich end of the compositional range in Figure 1 with the composition $Fe_{57.0}S_{43.0}$.

The composition of $Fe_{1-x}S$ changes substantially in the various associations, becoming richer in S and Pt with increasing fugacity of sulfur. Its compositional field follows the Fe–S join: $Fe_{49.5}S_{50.5}$ (0.02 wt% Pt measured), $Fe_{49.3}S_{50.7}$ (0.01 wt% Pt) and $Fe_{49.4}S_{50.6}$ (0.03 wt% Pt) for the associations po – (Fe,S) melt – γ(Fe,Pt), po – γ(Fe,Pt), po – γ(Fe,Pt) – PtFe, respectively. In all these runs, the measured Pt content in $Fe_{1-x}S$ is less than the detection limit of the electron microprobe. The monosulfide solid-solution (*mss*) $Fe_{48.2}S_{52.8}$ associated with PtFe and Pt_3Fe still contains no detectable Pt (0.03 wt%). However, the composition of $Fe_{1-x}S$ in the ternary association with Pt_3Fe and PtS is $Fe_{46.7(5)}Pt_{0.4(1)}S_{52.9(7)}$ (average of mutually very close values from seven runs). The *mss* composition in the binary association with PtS follows a path shown in Figure 1. We have analyzed the part of the binary join richest in sulfur where the Pt content in *mss* was found to vary between 0.87 and 1.11 at.%. The average composition of this *mss* is $Fe_{45.0(3)}Pt_{1.0(1)}S_{54.0(4)}$, and the composition richest in sulfur is $Fe_{44.7}Pt_{1.0}S_{54.3}$. During the quench, an unknown Pt-bearing phase exsolves as "dusting" from the originally homogeneous Pt-enriched monosulfide solid-solution. This phenomenon is clearly seen in the images obtained using back-scattered electrons (Fig. 2). Therefore, these samples were analyzed with a sweeping electron beam, 8–10 analyses being made of each sample.

The S-rich sulfide melt was analyzed with a rastered electron beam. On quenching, the melt yields dendritic aggregates of *mss* and a eutectic mixture of $Fe_{1-x}S$ and PtS. Because the quench product was relatively coarse, more than 30 area analyses were performed for each sample in order to obtain an average composition of the melt. Another difficulty arose owing to release of sulfur from the melt during quenching. As mentioned above, the melt composition was calculated as an intersection of a line passing through the measured composition of the PtS and that of original charge with a line with the fixed metal ratio, obtained from the analyses. The original composition of the melt in ternary association with PtS and S was estimated as $Fe_{31.7}Pt_{5.8}S_{62.5}$; sulfides in this charge were found to be intergrown with native sulfur. Only one attempt was made to estimate the composition of quench products. The average composition of the eutectic mixture after sulfur loss was found to be $Fe_{37.9}Pt_{7.5}S_{54.5}$, whereas several analyses of dendritic *mss* gave $Fe_{43.8}Pt_{0.8}S_{55.4}$.

Discussion

The phases prepared by direct synthesis is this study represent the most important Pt carriers in PGE deposits.

Pt–Fe alloys

The compositions of natural Pt–Fe alloys from placers are grouped around the values of 16–17 and 25 at.% (Fe,Cu,Ni) (Cabri *et al.* 1996) (Table 2). The composi-

TABLE 2. NATURAL Pt–Fe ALLOY COMPOSITIONS

Geological setting	Composition	Locality	Reference
placers	16–17 and ~25 at.% (Fe,Cu,Ni) *n* = 1709	Russia, Turkey, Brazil, *etc.*	Cabri *et al.* (1996)
ultramafic rocks, *e.g.*, dunite, harzburgite, lherzolite	24.6 at.% Fe *n* = 114	Alto Condoto complex, Colombia	Tistl (1994)
coarse-grained pyroxenite with chromitite layers	close to ideal Pt_3Fe	Impala mining area, Merensky Reef, Bushveld Complex, South Africa	Mostert *et al.* (1982)
chromite-bearing dunites	23.5 at.% (Fe,Ni,Cu) *n* = 20	Shantar Islands, Russia	Ivanov *et al.* (1995)
alkaline ultrabasic rocks	26.6 at.% (Fe,Cu,Ni) *n* = 615	Krasnogorskyi massif, Aldanskyi Shield, Russia	Mochalov *et al.* (1988)

n: number of analyses made.

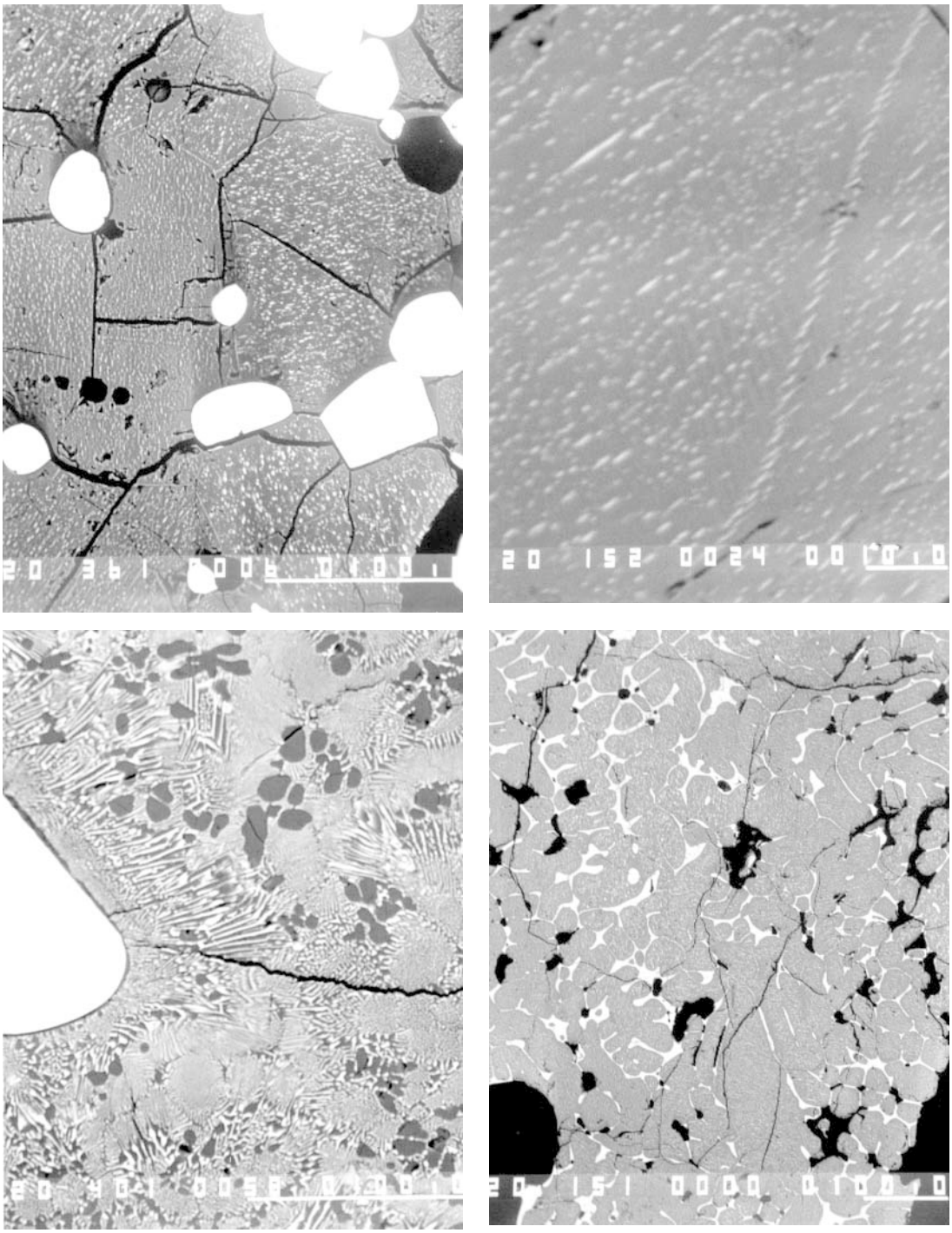

FIG. 2. a. Phase assemblage Pt-bearing pyrrhotite (with the Pt-rich phase exsolved) – PtS. Charge 11–C. Back-scattered electron (BSE) image. Scale bar: 100 μm. b. Detail of exsolution blebs of platinum in pyrrhotite. BSE image, charge 11–22. Scale bar: 10 μm. c. Solidified S-rich melt (pyrrhotite dendrites and a eutectic matrix) and a grain of associated PtS. Scale bar: 100 μm. d. The quench structure of a solidified S- and Fe-rich melt. Thickened dendrites of platiniferous pyrrhotite (with Pt-rich exsolution-induced blebs) and Pt-enriched interstitial liquid (white). Scale bar: 10 μm.

tion of the Pt–Fe alloys from Colombian ultramafic complexes clusters around 24.6 at.% Fe (Tistl 1994), although no cooperite was encountered in the samples. However, Cabri *et al.* (1996) reported cooperite inclusions in Pt–Fe alloys in placers derived from these massifs. The composition of the Pt–Fe alloy in the three-phase pyrrhotite – Pt_3Fe – PtS assemblage of the Merensky Reef ores approaches the ideal Pt_3Fe (Mostert *et al.* 1982). The average composition of the Pt–Fe alloy from Shantarskye Islands (Russia) is 23.5 at.% (Fe,Ni,Cu) (Ivanov *et al.* 1995); the Pt–Fe alloy from primary and placer accumulations from the Krasnogorskiy massif and Aldanskiy Shield (Russia) contains 26.6 at.% (Fe,Cu,Ni), on average (Mochalov *et al.* 1988). These findings correlate well with the fact that the ternary assemblage Pt_3Fe – *mss* – cooperite dominates the S-poor portion of the system Pt–Fe–S in all isothermal sections studied. The composition of the Pt–Fe alloy does not change significantly with temperature: $Fe_{27.5}Pt_{72.5}$ (900°C) (Makovicky *et al.* 1988), $Fe_{26.0}Pt_{74.0}$ (1000°C) (Skinner *et al.* 1976) and $Fe_{26.1}Pt_{73.9}$ at 1100°C. The alloy containing about 16–17 at.% Fe is probably the γ(Pt, Fe) composition richest in iron that is found in association with Pt_3Fe at temperatures lower than 900°C. This assemblage should be pyrrhotite-free, and typical of low-S associations.

In the natural Pt–Fe alloys, exsolution lamellae of osmium, as well as drop- and flame-like inclusions of iridium and rarer ruthenium, are documented from numerous PGE deposits from Russia, Turkey, Brazil and elsewhere (Cabri *et al.* 1996). The effect of these additional components, as well as that of surrounding silicates, on the equilibrium composition of the Pt–Fe alloys is poorly understood. A relevant publication by Makovicky & Karup-Møller (2000) exists on the alloys in the Pt–Ir–Fe–S system, indicating up to 5 at.% Ir in γ(Pt,Fe), 29.3 at.% Ir in Pt_3Fe, and 24.0 at.% Ir in PtFe at 1100°C. The occurrence of PtFe seems to be restricted to special environments, as exsolution blebs [together with Pt_2FeCu and (Pt,Fe,Ni)] in Pt_3Fe (Mochalov *et al.* 1988) or, more commonly, as a product of low-temperature (hydrothermal?) alteration of Pt_3Fe (*e.g.*, Ivanov *et al.* 1995, Cabri *et al.* 1996).

Cooperite

Makovicky *et al.* (1988) reported an increase in the Fe content of cooperite associated with Pt_3Fe as a function of falling temperature. It was determined as 1.1 at.% at 900°C and 1.9 at.% at 500°C. Skinner *et al.* (1976) found that at 1000°C, PtS dissolves no more than 0.5 at.% Fe, but Bryukvin *et al.* (1987) reported 3.9 at.% Fe in PtS at 1095°C. Our data indicate 0.5–0.7 at.% Fe in PtS associated with Pt_3Fe and $Fe_{1-x}S$ at 1100°C. A similar trend of increasing solubility of the minor component has been described for Ni in PdS (Karup-Møller & Makovicky 1993), Fe in PdS (Makovicky & Karup-Møller 1993), and Fe in Ir_2S_3 (Makovicky & Karup-Møller 2000). A mild positive correlation ($r = 0.4990$, $n = 23$) was found between the Fe content in cooperite and Ni content in braggite, in intergrown grains (Verryn & Merkle 1994), which may corroborate this trend in natural material. The extensive database of Cabri *et al.* (1996) shows an exceptional, single maximum Fe content of 4.33 at.% in cooperite, with other rare samples reaching 1.6 at.% Fe. The Fe content in the bulk of the cooperite samples, however, is mostly zero, with a small group between 0.3–0.5 at.% Fe. Johan *et al.* (1989) described cooperite crystals from Fifield, Australia, that formed before the end of crystallization of clinopyroxene and reacted at high temperatures to form complex intergrowths with Pt_3Fe. Petrographic observations and the low Fe content (0.1 at.%) imply the formation of cooperite at early stages of ore deposition.

In the Merensky Reef, Mostert *et al.* (1982) distinguished two types of cooperite: the first one is rich in Ir (~2 wt.%), and the other, virtually iridium-free. The former type contains appreciable amounts of Fe (1.7, 4.4 at.%), whereas the latter, only 0.2 at.%. Unfortunately, results of only three analyses of cooperite among hundreds of PGM analyses performed in their study were tabulated, so that no rigorous evaluation of Fe content in the two types of cooperite can be made. Mostert *et al.* (1982) interpreted the origin of the Pt–Fe alloy in the Merensky Reef as being high-temperature and magmatic, with cooperite formed by reaction of the alloy with the surrounding sulfide liquid at 1000°C or more. However, the elevated Fe and Ir content in the first type of cooperite suggests that at least a part of PtS crystallized later. The later action of hydrothermal fluids is well documented in both sulfide and silicate assemblages (Mostert *et al.* 1982). Evstigneeva & Tarkian (1996) were able to recrystallize pyrrhotite, PtS and PtFe alloys in their hydrothermal experiments at temperatures in the range 240–500°C.

Pyrrhotite

Maximal solubility of Pt in $Fe_{1-x}S$ increases with increasing temperature from practically nil at 500°C through 0.6 at.% at 900°C to 1.1 at.% at 1100°C. The latter value is equivalent to 5 wt.% Pt. Stoichiometric iron monosulfide was found not to dissolve Pt. Increasing deviation from the stoichiometric formula increases the ability of the phase to accommodate Pt (Bryukvin *et al.* 1987, Makovicky *et al.* 1986, 1988). A significant portion of the dissolved Pt exsolves on cooling, even in the case of rapid quenching (Makovicky *et al.* 1988, this work). In nature, the exsolved Pt is expected to be remobilized by Cl-rich fluids or late sulfidic melts and redistributed, resulting in pyrrhotite with only trace amounts of Pt or none at all (Makovicky *et al.* 1986, Molnar *et al.* 1997). McLaren & de Villiers (1982) found a rim of Pt–Fe alloy on pyrrhotite in many samples, and suggested that it represents a product of exsolution. Kingston & El-Dosuky (1982) described a

symplectitic intergrowth of Pt–Fe alloy with base-metal sulfides, mostly with pyrrhotite, and interpreted it as a result of segregation of Pt during *mss* decomposition, leading to a continuum between fine and coarse intergrowths. The bulk composition of this type of alloy was not obtained owing to analytical difficulties. The nature of these intergrowths is still controversial, however. The presence of pyrrhotite enriched in Pt was mentioned by Distler (1994) and also assumed by Kingston & El-Dosuky (1982), who favored the idea of solid solution of PGE or the presence of submicroscopic PGM of colloidal size in base-metal sulfides, on the basis of calculations of the bulk chemical composition of the Merensky Reef ore.

S-rich melt

The S-rich sulfide melt observed in this study is able to dissolve a substantial amount of Pt (7.5 at.%, *i.e.*, up to 27.5 wt.% Pt; calculated for the S-depleted product of solidification with 54.3 at.% S). The exact S content in the melt can only be obtained by the extrapolations described above. Such calculations allow us to ascertain the S contents of the liquid in the charges F and E in Table 1 as 60.6 and 61.4 at.%, respectively; those of charges A, B and C were set to 60+ at.% S. The S-rich limit of the melt remains uncertain; charge E contains native S mixed with sulfides, suggesting that this limit lies at 62–63 at.% S. Bryukvin *et al.* (1987) described a ternary eutectic point between $FeS_{1.09}$, Pt_3Fe and PtS at ~1050 ± 10°C with the composition $Fe_{32.3}Pt_{23.7}S_{44.0}$, and a eutectic point on the pseudobinary join $FeS_{1.09}$–PtS at 1095 ± 10°C with the composition $Fe_{35.6}Pt_{11.5}S_{52.9}$, quoted as $Fe_{35}Pt_{14}S_{51}$ in Raghavan (1988). None of these melts were encountered in the present study; the corresponding melts enriched in Ir were found in the quaternary phase system Pt–Ir–Fe–S at 1100°C by Makovicky & Karup-Møller (2000).

Conclusions

1. The solubility of platinum in pyrrhotite increases with increasing temperature from nil at 500°C and 2.7 wt.% at 900°C to 5.0 wt.% at 1100°C. Stoichiometric FeS does not dissolve Pt; increasing deviation from the stoichiometric formula increases the ability of pyrrhotite to accommodate Pt. A significant portion of Pt dissolved in $Fe_{1-x}S$ in our experimental charges exsolves during the quench. In natural conditions, the exsolved platinum is remobilized by later fluids or sulfidic melts and redistributed, resulting in pyrrhotite with only trace amounts of Pt or none at all.

2. In all isothermal sections studied, the sulfur-poor part of the phase diagram is dominated by the assemblage pyrrhotite – isoferroplatinum – cooperite. The composition of the Pt–Fe alloy in this assemblage does not change significantly with increasing temperature: $Fe_{27.5}Pt_{72.5}$ (900°C) (Makovicky *et al.* 1988), $Fe_{26.0}Pt_{74.0}$ (1000°C) (Skinner *et al.* 1976), and $Fe_{26.1}Pt_{73.9}$ (1100°C, this study). Therefore, the alloy compositionally close to Pt_3Fe will be of little use as a geothermometer.

Most of the published material shows that the composition of the natural Pt–Fe alloy is close to Pt_3Fe, indicating the ubiquitous presence of the assemblage isoferroplatinum – cooperite – pyrrhotite. Our experimental data suggest, however, that alloy grains with a composition of about 16–17 at.% Fe, reported by Cabri *et al.* (1996) from placer deposits, were formed in a pyrrhotite-free assemblage. We are not aware of a report on tetraferroplatinum as an early high-temperature phase.

3. Experimental data on the composition of cooperite in the system Pt–Fe–S suggest that the Fe content of cooperite associated with the alloy Pt_3Fe increases with falling temperature, from 0.5–0.7 at.% at 1100°C to 1.9 at.% at 500°C. Assuming that the chemical composition of cooperite was not modified after its formation, its iron content can be used as a rough guide to estimate the temperature of crystallization.

4. The Fe-rich sulfide melt does not dissolve platinum, whereas the S-rich sulfide melt observed in this study is able to dissolve substantial amounts of Pt (23.1 wt.%). The eutectic melts defined by Bryukvin *et al.* (1987) were not encountered in the present study.

Acknowledgements

This paper is dedicated to Dr. Louis J. Cabri, one of the founders of PGE mineralogy, with thanks for his tireless assistance to us and everybody else tackling the problems concerning the PGE minerals. This project was supported by the Danish Rectors' Conference, the University of Copenhagen, the University of Bratislava and the University of California (Davis). Active interest of Doc. Dr. M. Chovan (Bratislava) and Doc. Dr. S. Karup-Møller (Danish Technical University), as well as the professional help of Mr. J. Fløng and Mrs. C. Sarantaris, and the assistance of two anonymous referees and of Robert F. Martin, are gratefully acknowledged.

References

Bowles, J.F.W. (1990): Platinum–iron alloys, their structural and magnetic characteristics in relation to hydrothermal and low-temperature genesis. *Mineral. Petrol.* **43**, 37-47.

Bryukvin, V.A., Fishman, B.A., Reznichenko, V.A., Shekhter, L.N., Blokhina, L.I. & Kukoyev, V.A. (1987): Studies on the phase diagram of the Fe–Pt–S system. *Izv. Akad. Nauk SSSR, Metally* **1987**(4), 25-30 (in Russ.).

_____, Shekhter, L.N., Reznichenko, V.A., Blokhina, L.I. & Kukoyev, V.A. (1985): On phase equilibrium in the system Pt–PtS. *Izv. Akad. Nauk SSSR, Metally* **1985**(5), 191-192 (in Russ.).

CABRI, L.J. & FEATHER, C.E. (1975): Platinum–iron alloys: a nomenclature based on a study of natural and synthetic alloys. *Can. Mineral.* **13**, 117-126.

_____, HARRIS, D.C. & WEISER, T.W. (1996): Mineralogy and distribution of platinum-group mineral (PGM) placer deposits of the world. *Explor. Mining Geol.* **5**, 73-167.

DISTLER, V.V. (1994): Platinum mineralization of the Noril'sk deposits. *In* Proc. Sudbury–Noril'sk Symposium (P.C. Lightfoot & A.J. Naldrett, eds.). *Ontario Geol. Surv., Spec. Vol.* **5**, 243-260.

EVSTIGNEEVA, T. & TARKIAN, M. (1996): Synthesis of platinum-group minerals under hydrothermal conditions. *Eur. J. Mineral.* **8**, 549-564.

IVANOV, V.V., LENNIKOV, A.M., NEKRASOV, I.YA., OKTYABRSKIY, R.A., KHITROV, V.V., SAPIN, V.I., TASKAYEV, V.I., VETOSHKEVICH, A.D. & MOLCHANOVA, G.B. (1995): Chrome spinel and mineralization of platinum metals in the Feklistovsk dunite and clinopyroxenite massif, Shantar Island, Okhotsk Sea region. *Geologiya Rudnykh Mestorozhdeniy* **37**(1), 77-83 (in Russ.).

JOHAN, Z., OHNENSTETTER, M., SLANSKY, E., BARRON, L.M. & SUPPEL, D. (1989): Platinum mineralization in the Alaskan-type intrusive complexes near Fifield, New South Wales, Australia. 1. Platinum-group minerals in clinopyroxenites of the Kelvin Grove prospect, Owendale intrusion. *Mineral. Petrol.* **40**, 289-309.

KARUP-MØLLER, S. & MAKOVICKY, E. (1993): The system Pd–Ni–S at 900°, 725°, 550°, and 400°C. *Econ. Geol.* **88**, 1261-1268.

KINGSTON, G.A. & EL-DOSUKY, B.T. (1982): A contribution on the platinum-group mineralogy of the Merensky Reef at the Rustenburg Platinum Mine. *Econ. Geol.* **77**, 1367-1384.

KUBASCHEWSKI, O. (1982): Iron–sulphur. *In* Iron – Binary Phase Diagrams. Springer-Verlag, Berlin, Germany (125-128).

MAKOVICKY, E. & KARUP-MØLLER, S. (1993): The system Pd–Fe–S at 900°, 725°, 550°, and 400°C. *Econ. Geol.* **88**, 1269-1278.

_____ & _____ (2000): Phase relations in the metal-rich portions of the phase system Pt–Ir–Fe–S at 1000°C and 1100°C. *Mineral. Mag.* **64**, 1047-1056.

MAKOVICKY, M., MAKOVICKY, E. & ROSE-HANSEN, J. (1986): Experimental studies on the solubility and distribution of platinum group elements in base-metal sulphides in platinum deposits. *In* Metallogeny of Basic and Ultrabasic Rocks (M.J. Gallagher, R.A. Ixer, C.R. Neary & H.M. Prichard, eds.). The Institution of Mining and Metallurgy, London, U.K. (415-425).

_____, _____ & _____ (1988): Experimental evidence of the formation and mineralogy of platinum and palladium ore deposits. *In* Mineral Deposits within the European Community (J. Boissonnas & P. Omenetto, eds.). Springer-Verlag, Berlin, Germany (303-317).

_____, _____ & _____ (1992): The phase system Pt–Fe–As–S at 850°C and 470°C. *Neues Jahrb. Mineral., Monatsh.*, 441-453.

MCLAREN, C.H. & DE VILLIERS, J.P.R. (1982): The platinum group chemistry and mineralogy of the UG–2 chromitite layer of the Bushveld Complex. *Econ. Geol.* **77**, 1348-1366.

MOCHALOV, A.G., ZHERNOVSKIY, I.V. & DMITRENKO, G.G. (1988): Composition and distribution of native platinum and iron minerals in ultrabasites. *Geologiya Rudnykh Mestorozhdeniy* **30**(5), 47-58 (in Russ.).

MOLNAR, F., WATKINSON, D.H., JONES, P.C. & GATTER, I. (1997): Fluid inclusion evidence for hydrothermal enrichment of magmatic ore at the contact zone of the Ni–Cu–platinum-group element 4b deposit, Lindsley mine, Sudbury, Canada. *Econ. Geol.* **92**, 674-685.

MOSTERT, A.B., HOFMEYR, P.K. & POTGIETER, G.A. (1982): The platinum-group mineralogy of the Merensky Reef at the Impala Platinum Mines, Bophuthatswana. *Econ. Geol.* **77**, 1385-1394.

RAGHAVAN, V. (1988): *Phase Diagrams of Ternary Iron Alloys. 2. Ternary Systems Containing Iron and Sulphur*. The Indian Institute of Metals, Calcutta, India.

SKINNER, B.J., LUCE, F.D., DILL, J.A., ELLIS, D.E., HAGAN, H.A., LEWIS, D.M., ODELL, D.A., SVERJENSKY, D.A. & WILLIAMS, N. (1976): Phase relations in ternary portions of the systems Pt–Pd–Fe–As–S. *Econ. Geol.* **71**, 1469-1475.

TISTL, M. (1994): Geochemistry of platinum-group elements of the zoned ultramafic Alto Condoto complex, northwest Colombia. *Econ. Geol.* **89**, 158-167.

VERRYN, S.M.C. & MERKLE, R.K.W. (1994): Compositional variation of cooperite, braggite and vysotskite from the Bushveld Complex. *Mineral. Mag.* **58**, 223-234.

Received May 4, 2000, revised manuscript accepted October 15, 2001.